

Large-scale dynamics of self-propelled particles moving through obstacles: How environment affects particle swarms

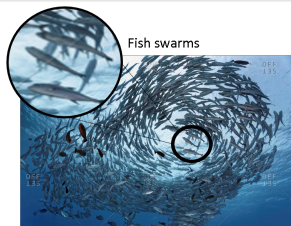
Diane PEURICHARD
INRIA Paris, team MAMBA

In collaboration with:

P. DEGOND - IMT, Toulouse
A. MANHART - Wien University
S. MERINO - Wien University
P. ACEVES-SANCHEZ - UCLA
E. KEAVENY - IMFT, Toulouse
L. SALA - INRAE



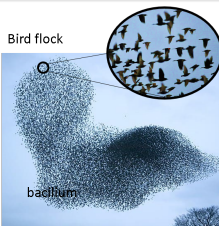
Collective motion: Examples in nature



Fish swarms

Swarm Bigeye trevallies (*Caranx sexfasciatus*) in the blue water, Pacific, French Polynesia, Oceania

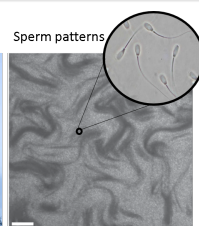
Credit: Norbert Probst / [ImageBROKER](#)



Bird flock

Starlings flying to roost near Kendal in Cumbria, UK.

Credit: Ashley Cooper / The Image Bank / Getty



Sperm patterns

Creppey et al. Turbulence of swarming sperm.

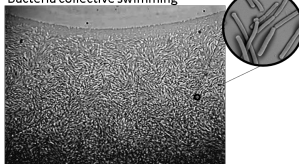
Phys. Rev. E. (2015)

Pedestrian crowds, lanes



Johansson et al. Crowd and environmental management during mass gatherings
The Lancet infectious diseases (2012)

Bacteria collective swimming



L. H. Cisneros, et al. Fluid dynamics of self-propelled microorganisms, from individuals to concentrated populations.
Experiments in Fluids, 43:737-753, 2007.

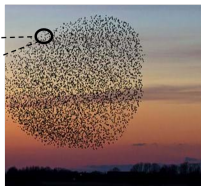
- Self-organization: Emergence of large-scale ordered structures from local, small-scale interactions

Mathematical modelling: Choosing the right scale

Microscopic scale



Macroscopic scale



	Microscopic scale	Macroscopic scale
Variables	Agents positions, speed	Mean variables (density, orientation etc)
Model type	ODE systems (N equations)	PDE equations/systems
Advantages	<ul style="list-style-type: none"> - Modelling precision - Link with experimental data 	<ul style="list-style-type: none"> - Theoretical analysis - Computational efficiency
Drawbacks	<ul style="list-style-type: none"> - Lack of theoretical results - Computationally challenging 	- Loss of informations at the agent's scale
References	[Vicsek et al. (1995)], [Cucker and Smale. (2007)], [[S Bernardi, A Colombi, M Scianna (2018)] (swarms) [A. Kamal and E. E. Keaveny (2018)]	[J. A. Carrillo, Y.-P. Choi, S. Pérez (2017)], [J. A. Carrillo, D. Kalise, F. Rossi, E. Trélat (2022)] (flocks) [P. Degond, A. Manhart, and H. Yu (2018)] (alignment) [P. Degond, S. Merino-Aceituno, F. Vergnet, and H. Yu (2019)] [B. Maury, A. Roudneff-Chupin, and F. Santambrogio (2010)] (crowds) [M Burger, S Hittmeir, H Ranetbauer, MT Wolfram (2016)] (lane formation) [F. Othmer, K.J. Painter (2009)] (chemotaxis)

Mean-field: [Boley, Canizo, Carrillo (2011)], [J. A. Carrillo, Y.-P. Choi, M. Hauray (2014)]

Hydrodynamic limits: [Helbing (2001)], [Aw, Klar, Rascle, Materne (2002)], [Jiang, Xiong, Zhang (2016)], [Degond, Motsch (2008)], [Degond, Frouvelle, Liu (2012)], [Aceves-Sanchez, Bostan, Carrillo, Degond (2019)], [J.A Carrillo, M. Fornasier, J. Rosado, G. Toscani (2010)]

Diffusion limits: [HG Othmer, T Hillen (2000)]

Kinetic models: [Calvez, V., Gosse, L. and Twarogowska, (2017)], [Peruani and Markus Bär 2013 New J. Phys. (2013)].

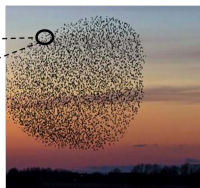
[Carrillo, D'Orsogna, Panferov (2009)]

Mathematical modelling: Choosing the right scale

Microscopic scale



Macroscopic scale



	Microscopic scale	Macroscopic scale
Variables	Agents positions, speed	Mean variables (density, orientation etc)
Model type	ODE systems (N equations)	PDE equations/systems
Advantages	<ul style="list-style-type: none"> - Modelling precision - Link with experimental data 	<ul style="list-style-type: none"> - Theoretical analysis - Computational efficiency
Drawbacks	<ul style="list-style-type: none"> - Lack of theoretical results - Computationally challenging 	<ul style="list-style-type: none"> - Loss of informations at the agent's scale
References	[Vicsek et al. (1995)], [Cucker and Smale. (2007)], [[S Bernardi, A Colombi, M Scianna (2018)] (swarms) (A. Kamal and E. E. Keaveny (2018)) Swimmers in obstacles	[J. A. Carrillo, Y.-P. Choi, S. Pérez (2017), J. A. Carrillo, D. Kalise, F. Rossi, E. Trélat (2022)] (flocks) [P. Degond, A. Manhart, and H. Yu (2018)] (alignment) Swimmers in viscous fluid [P. Degond, S. Merino-Aceituno, F. Vergnet, and H. Yu (2019)] [B. Maury, A. Roudneff-Chupin, and F. Santambrogio (2010)] (crowds) [M Burger, S Hittmeir, H Ranetbauer, MT Wolfram (2016)] (lane formation) [K. Han, K.J. Painter (2009)] (chemotaxis)

Mean-field: [Boley, Canizo, Carrillo (2011)], [J. A. Carrillo, Y.-P. Choi, M. Hauray (2014)]

Hydrodynamic limits: [Helbing (2001)], [Aw, Klar, Rascle, Materne (2002)], [Jiang, Xiong, Zhang (2016)], [Degond, Motsch (2008)], [Degond, Frouvelle, Liu (2012)],

[Aceves-Sanchez, Bostan, Carrillo, Degond (2019)], [J.A Carrillo, M. Fornasier, J. Rosado, G. Toscani (2010)]

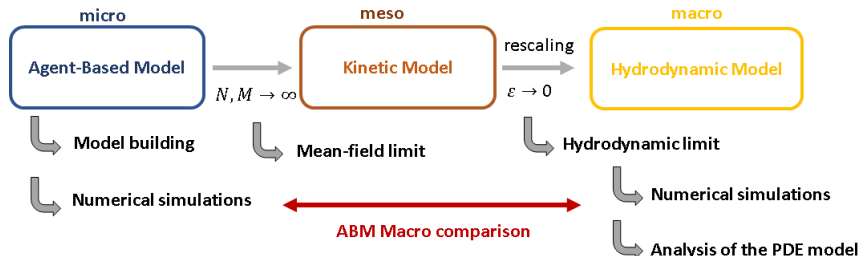
Diffusion limits: [HG Othmer, T Hillen (2000)]

Kinetic models: [Calvez, V., Gosse, L. and Twarogowska, (2017)], [Peruani and Markus Bär 2013 New J. Phys. (2013)],

[Carrillo, D'Orsogna, Panferov (2009)]

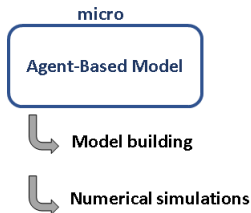
Plan of the talk

Objectives: Investigate pattern emergence using ABM and PDE



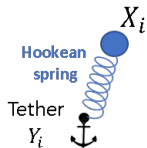
Plan of the talk

Objectives: Investigate pattern emergence using ABM and PDE



Agent-based model

Obstacles



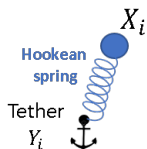
Swimmers



- Obstacles: Centers $X_i(t) \in \mathbb{R}^2$, $i = 1 \dots N$ attached to anchor points $Y_i \in \mathbb{R}^2$ via hookean springs
- Swimmers: Centers $Z_k(t) \in \mathbb{R}^2$, self-propelled along orientation vectors $\alpha_k(t) \in \mathbb{S}^1$, $k = 1 \dots M$

Agent-based model

Obstacles



Swimmers



- Obstacles: Centers $X_i(t) \in \mathbb{R}^2$, $i = 1 \dots N$ attached to anchor points $Y_i \in \mathbb{R}^2$ via hookean springs
- Swimmers: Centers $Z_k(t) \in \mathbb{R}^2$, self-propelled along orientation vectors $\alpha_k(t) \in \mathbb{S}^1$, $k = 1 \dots M$

Equations of motion (Newton overdamped):

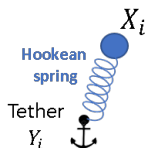
$$dX_i = -\frac{\kappa}{\eta}(X_i - Y_i)dt - \frac{1}{\eta} \frac{1}{M} \sum_{k=1}^M \nabla \phi(X_i - Z_k) dt + \sqrt{2d_o} dB_t^i,$$

$$dZ_k = u_0 \alpha_k dt - \frac{1}{\zeta} \frac{1}{N} \sum_{i=1}^N \nabla \phi(Z_k - X_i) dt - \frac{1}{\zeta} \frac{1}{M} \sum_{l \neq k}^M \nabla \psi(Z_k - Z_l) dt,$$

$$d\alpha_k = P_{\alpha_k^\perp} \circ \left[\nu \bar{\alpha}_k dt + \sqrt{2d_s} d\tilde{B}_t^k \right]$$

Agent-based model

Obstacles



Swimmers



- Obstacles: Centers $X_i(t) \in \mathbb{R}^2$, $i = 1 \dots N$ attached to anchor points $Y_i \in \mathbb{R}^2$ via hookean springs
- Swimmers: Centers $Z_k(t) \in \mathbb{R}^2$, self-propelled along orientation vectors $\alpha_k(t) \in \mathbb{S}^1$, $k = 1 \dots M$

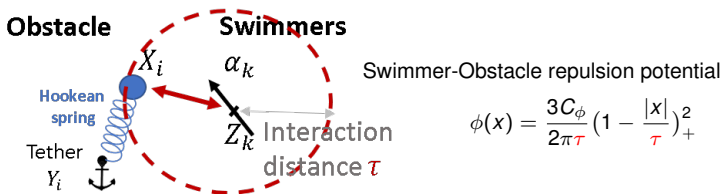
Equations of motion (Newton overdamped):

$$dX_i = -\frac{\kappa}{\eta}(X_i - Y_i)dt - \frac{1}{\eta} \frac{1}{M} \sum_{k=1}^M \nabla \phi(X_i - Z_k) dt + \overbrace{\sqrt{2d_o} dB_t^i}^{\text{Brownian noise}},$$

$$dZ_k = u_0 \alpha_k dt - \frac{1}{\zeta} \frac{1}{N} \sum_{i=1}^N \nabla \phi(Z_k - X_i) dt - \frac{1}{\zeta} \frac{1}{M} \sum_{l \neq k}^M \nabla \psi(Z_k - Z_l) dt,$$

$$d\alpha_k = P_{\alpha_k^\perp} \circ \left[\nu \bar{\alpha}_k dt + \sqrt{2d_s} dB_t^k \right]$$

Agent-based model



Equations of motion (Newton overdamped):

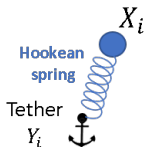
$$dX_i = -\frac{\kappa}{\eta}(X_i - Y_i)dt - \overbrace{\frac{1}{\eta} \frac{1}{M} \sum_{k=1}^M \nabla \phi(X_i - Z_k)}^{\text{Sw-Ob repulsion}} dt + \sqrt{2d_o} dB_t^i,$$

$$dZ_k = u_0 \alpha_k dt - \frac{1}{\zeta} \frac{1}{N} \sum_{i=1}^N \nabla \phi(Z_k - X_i) dt - \frac{1}{\zeta} \frac{1}{M} \sum_{l \neq k}^M \nabla \psi(Z_k - Z_l) dt,$$

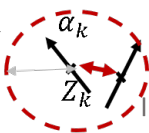
$$d\alpha_k = P_{\alpha_k^\perp} \circ \left[\nu \bar{\alpha}_k dt + \sqrt{2d_s} d\tilde{B}_t^k \right]$$

Agent-based model

Obstacle



Swimmers



Swimmer-Swimmer repulsion potential

$$\psi(x) = \frac{6\mu}{\pi r_R^2} \left(1 - \frac{|x|}{r_R}\right)_+^2$$

Interaction
distance r_R

Equations of motion (Newton overdamped):

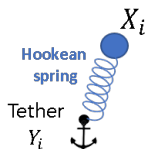
$$dX_i = -\frac{\kappa}{\eta}(X_i - Y_i)dt - \frac{1}{\eta} \frac{1}{M} \sum_{k=1}^M \nabla \phi(X_i - Z_k) dt + \sqrt{2d_o} dB_t^i,$$

$$dZ_k = u_0 \alpha_k dt - \frac{1}{\zeta} \frac{1}{N} \sum_{i=1}^N \nabla \phi(Z_k - X_i) dt - \underbrace{\frac{1}{\zeta} \frac{1}{M} \sum_{l \neq k}^M \nabla \psi(Z_k - Z_l) dt}_{\text{Sw-Sw repulsion}},$$

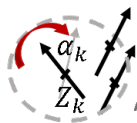
$$d\alpha_k = P_{\alpha_k^\perp} \circ \left[\nu \bar{\alpha}_k dt + \sqrt{2d_s} d\tilde{B}_t^k \right]$$

Agent-based model

Obstacle



Swimmers



Swimmer-Swimmer alignment

$$\bar{\alpha}_k = \frac{J_k}{|J_k|}, \quad J_k = \sum_{j=1, |Z_k - Z_j| \leq r_A}^M \alpha_j$$

Alignment
distance r_A

Equations of motion (Newton overdamped):

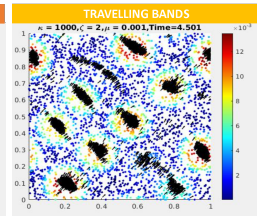
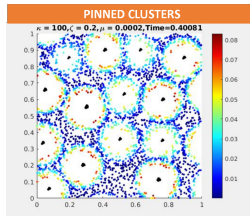
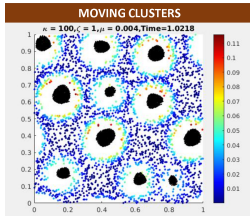
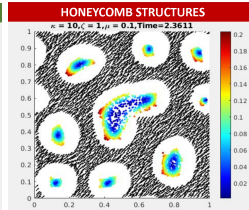
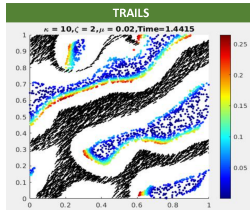
$$dX_i = -\frac{\kappa}{\eta}(X_i - Y_i)dt - \frac{1}{\eta} \frac{1}{M} \sum_{k=1}^M \nabla \phi(X_i - Z_k) dt + \sqrt{2d_o} dB_t^i,$$

$$dZ_k = u_0 \alpha_k dt - \frac{1}{\zeta} \frac{1}{N} \sum_{i=1}^N \nabla \phi(Z_k - X_i) dt - \frac{1}{\zeta} \frac{1}{M} \sum_{l \neq k}^M \nabla \psi(Z_k - Z_l) dt,$$

Sw-Sw alignment

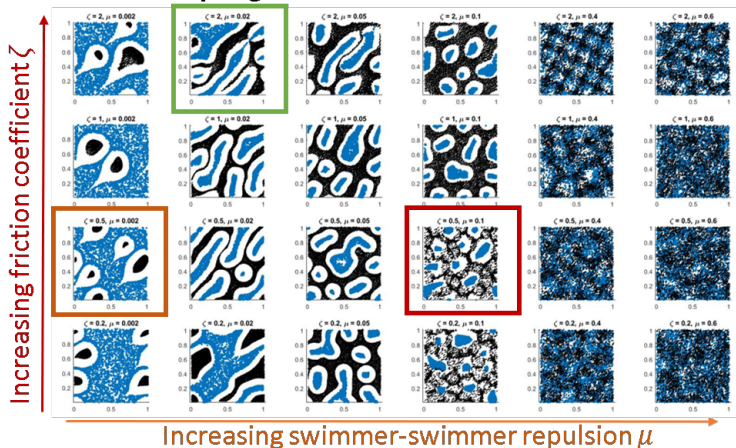
$$d\alpha_k = P_{\alpha_k^\perp} \circ \left[\overbrace{\nu \bar{\alpha}_k dt}^{\text{Sw-Sw alignment}} + \sqrt{2d_s} d\tilde{B}_t^k \right],$$

Numerical simulations - patterns



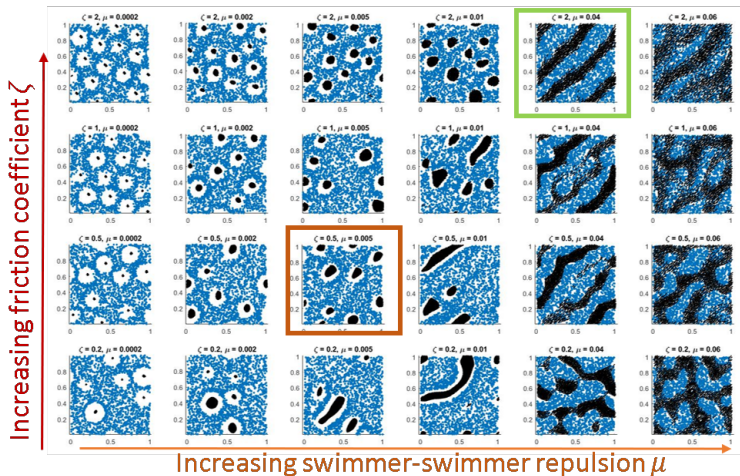
Numerical simulations - Weak obstacle spring stiffness

(A) Weak obstacle spring stiffness $\kappa = 10$



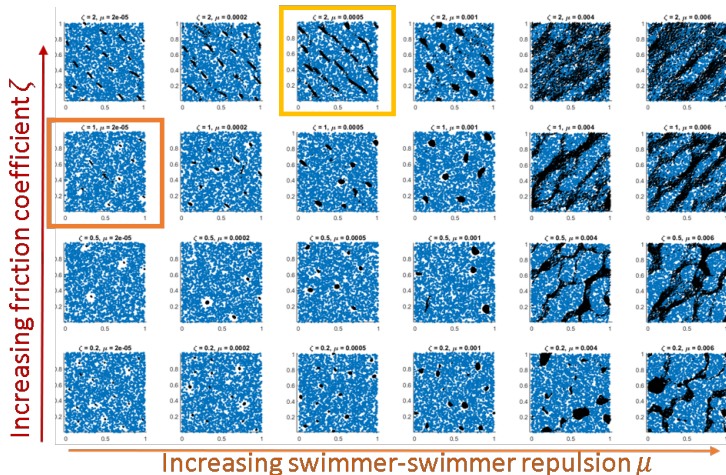
Numerical simulations - Mild obstacle spring stiffness

(B) Mild obstacle spring stiffness $\kappa = 100$

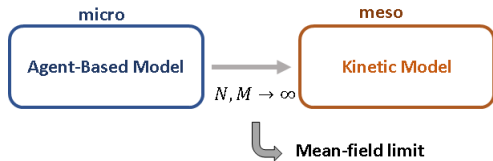


Numerical simulations - Strong obstacle spring stiffness

(C) Strong obstacle spring stiffness $\kappa = 10^3$



Derivation of a kinetic model in the limit $N, M \rightarrow \infty$



Distribution functions:

- $g^M(x, \alpha, t)$: density distribution of the M swimmers
- $f^N(x, y, t)$: density distribution of the N obstacles

Hydrodynamic model



Scaling assumptions:

- Scaling assumptions for the swimmers:
 - Small swimmer-swimmer alignment radius : $r_A = O(\varepsilon)$
 - Small swimmer-swimmer repulsion distance: $r_R = O(\varepsilon)$
 - Swimmer alignment rate and orientational noise intensity large: $d_s, \nu = O(\frac{1}{\varepsilon}), \frac{d_s}{\nu} = O(1)$
- Scaling assumptions for the obstacles:
 - Uniform anchor density $\rho_A \equiv 1$
 - Stiff springs: $\gamma = \frac{\eta}{\kappa} \ll 1$
 - Low obstacle noise: $d = d_0 \gamma \ll 1$

Hydrodynamic model



Scaling assumptions:

- Scaling assumptions for the swimmers:
 - Small swimmer-swimmer alignment radius : $r_A = O(\varepsilon)$
 - Small swimmer-swimmer repulsion distance: $r_R = O(\varepsilon)$
 - Swimmer alignment rate and orientational noise intensity large: $d_s, \nu = O(\frac{1}{\varepsilon}), \frac{d_s}{\nu} = O(1)$
- Scaling assumptions for the obstacles:
 - Uniform anchor density $\rho_A \equiv 1$
 - Stiff springs: $\gamma = \frac{\eta}{\kappa} \ll 1$
 - Low obstacle noise: $d = d_0 \gamma \ll 1$

Hydrodynamic model



Scaling assumptions:

- Scaling assumptions for the swimmers:
 - Small swimmer-swimmer alignment radius : $r_A = O(\varepsilon)$
 - Small swimmer-swimmer repulsion distance: $r_R = O(\varepsilon)$
 - Swimmer alignment rate and orientational noise intensity large: $d_s, \nu = O(\frac{1}{\varepsilon}), \frac{d_s}{\nu} = O(1)$
- Scaling assumptions for the obstacles:
 - Uniform anchor density $\rho_A \equiv 1$
 - Stiff springs: $\gamma = \frac{\eta}{\kappa} \ll 1$
 - Low obstacle noise: $d = d_0 \gamma \ll 1$

Observables:

- $\rho_g(x, t)$: local density of the swimmers
- $\Omega(x, t)$: local orientation of the swimmers
- $\rho_f(x, t)$: local density of the obstacles

Theorem (Macroscopic model)

The macroscopic swimmer density ρ_g and orientation Ω fulfil:

$$\begin{aligned}\partial_t \rho_g + \nabla \cdot (U \rho_g) &= 0, \\ \rho_g \partial_t \Omega + \rho_g (V \cdot \nabla) \Omega + d_3 P_{\Omega^\perp} \nabla \rho_g &= 0,\end{aligned}$$

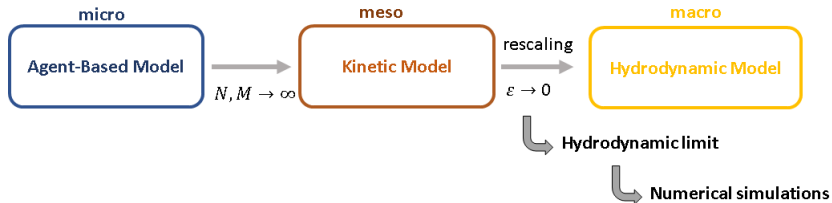
where

$$\begin{aligned}U &= d_1 \Omega - \frac{1}{\zeta} \nabla \bar{\rho}_f - \frac{\mu}{\zeta} \nabla \rho_g, \\ V &= d_2 \Omega - \frac{1}{\zeta} \nabla \bar{\rho}_f - \frac{\mu}{\zeta} \nabla \rho_g.\end{aligned}$$

Under assumptions $\gamma \ll 1$ and $\delta \ll 1$, the obstacle density $\rho_f(x, t)$ is given by:

$$\rho_f = 1 + \frac{\gamma}{\eta} \Delta \bar{\rho}_g - \frac{\gamma^2}{\eta} \partial_t \Delta \bar{\rho}_g + \frac{\gamma^2}{\eta^2} \mathcal{N}(\bar{\rho}_g) + \mathcal{O}(\gamma^3), \quad \mathcal{N}(\bar{\rho}_g) := \det^{\mathbb{H}}(\bar{\rho}_g),$$

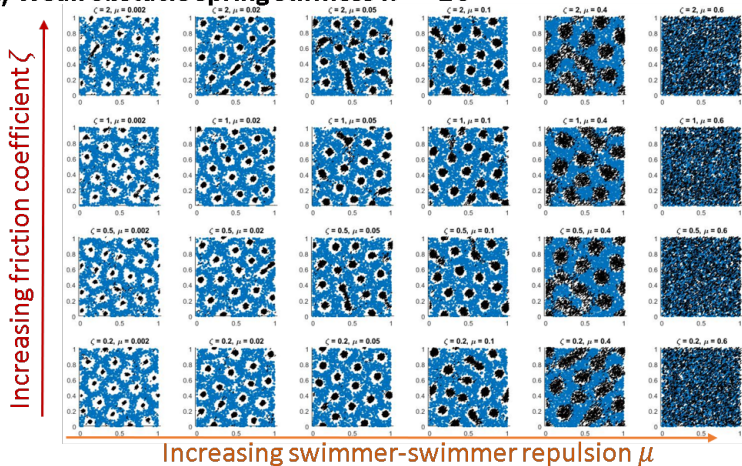
Numerical simulations of the macroscopic model



Numerical scheme adapted from [Motsch, Navoret, Mult. Mod. Simul., 2011],
[Carrillo, Chertock, Huang. Comm. in Comp. Phys., 2015]

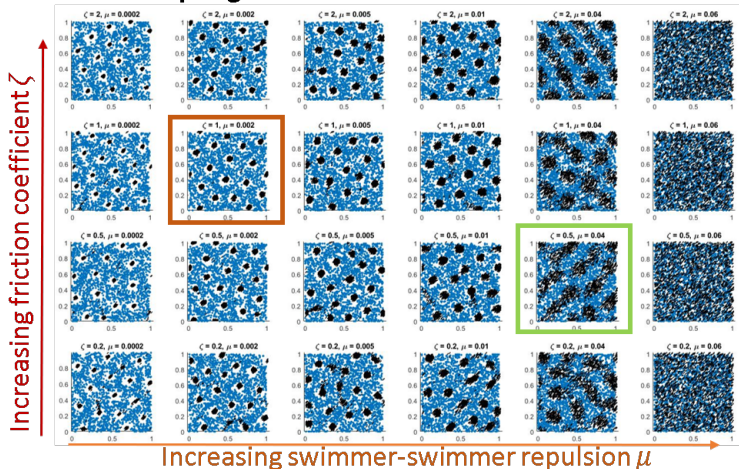
Numerical simulations - Weak obstacle spring stiffness

(A) Weak obstacle spring stiffness $\kappa = 10$



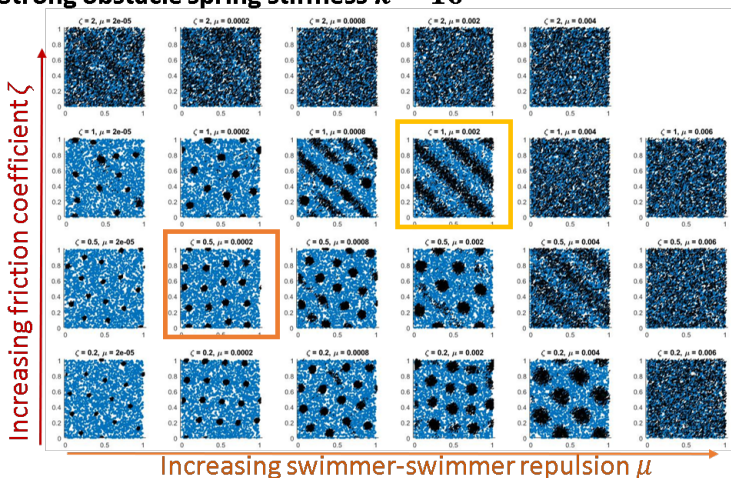
Numerical simulations - Mild obstacle spring stiffness

(B) Mild obstacle spring stiffness $\kappa = 100$

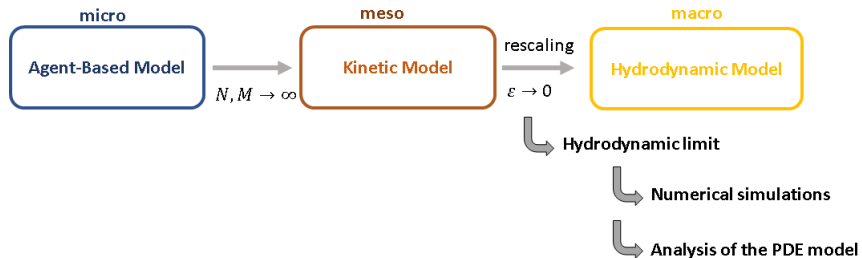


Numerical simulations - Strong obstacle spring stiffness

(C) Strong obstacle spring stiffness $\kappa = 10^3$



Numerical simulations - Mild obstacle spring stiffness



Linear stability analysis

- PDE system:

$$\partial_t \rho_g + \nabla \cdot \left((d_1 \Omega - \frac{1}{\zeta} \nabla \bar{\rho}_f - \frac{\mu}{\zeta} \nabla \rho_g) \rho_g \right) = 0,$$

$$\rho_g \partial_t \Omega + \rho_g \left((d_2 \Omega - \frac{1}{\zeta} \nabla \bar{\rho}_f - \frac{\mu}{\zeta} \nabla \rho_g) \cdot \nabla \right) \Omega + d_3 P_{\Omega^\perp} \nabla \rho_g = 0,$$

$$\rho_f = 1 + \frac{\gamma}{\eta} \Delta \bar{\rho}_g - \frac{\gamma^2}{\eta} \partial_t \Delta \bar{\rho}_g + \frac{\gamma^2}{\eta^2} \mathcal{N}(\bar{\rho}_g) + \mathcal{O}(\gamma^3),$$

- Linearize around (ρ_0, Ω_0) : $\rho_g = \rho_0 + \epsilon \rho_1 + \mathcal{O}(\epsilon^2)$, $\Omega = \Omega_0 + \epsilon \Omega_1 + \mathcal{O}(\epsilon^2)$

$$\partial_t \rho_1 + d_1 \Omega_0 \cdot \nabla \rho_1 + d_1 \rho_0 \nabla \cdot \Omega_1 = \bar{\mu} \rho_0 \Delta \rho_1 + \rho_0 \bar{\lambda} (\Delta^2 \bar{\rho}_1 - \gamma \Delta^2 \partial_t \bar{\rho}_1),$$

$$\rho_0 \partial_t \Omega_1 + \rho_0 d_2 (\Omega_0 \cdot \nabla) \Omega_1 + d_3 P_{\Omega_0^\perp} \nabla \rho_1 = 0,$$

$$\Omega_0 \cdot \Omega_1 = 0, \bar{\lambda} = \frac{\rho_A}{\kappa \zeta}$$

- Consider plane wave perturbations

$$\rho_1(x, t) = \bar{\rho} e^{ik \cdot x + \alpha t}, \quad \Omega_1(x, t) = \tilde{\Omega} e^{ik \cdot x + \alpha t}$$

Linear stability analysis

- PDE system:

$$\partial_t \rho_g + \nabla \cdot \left((d_1 \Omega - \frac{1}{\zeta} \nabla \bar{\rho}_f - \frac{\mu}{\zeta} \nabla \rho_g) \rho_g \right) = 0,$$

$$\rho_g \partial_t \Omega + \rho_g \left((d_2 \Omega - \frac{1}{\zeta} \nabla \bar{\rho}_f - \frac{\mu}{\zeta} \nabla \rho_g) \cdot \nabla \right) \Omega + d_3 P_{\Omega^\perp} \nabla \rho_g = 0,$$

$$\rho_f = 1 + \frac{\gamma}{\eta} \Delta \bar{\rho}_g - \frac{\gamma^2}{\eta} \partial_t \Delta \bar{\rho}_g + \frac{\gamma^2}{\eta^2} \mathcal{N}(\bar{\rho}_g) + \mathcal{O}(\gamma^3),$$

- Linearize around (ρ_0, Ω_0) : $\rho_g = \rho_0 + \epsilon \rho_1 + \mathcal{O}(\epsilon^2)$, $\Omega = \Omega_0 + \epsilon \Omega_1 + \mathcal{O}(\epsilon^2)$

$$\partial_t \rho_1 + d_1 \Omega_0 \cdot \nabla \rho_1 + d_1 \rho_0 \nabla \cdot \Omega_1 = \bar{\mu} \rho_0 \Delta \rho_1 + \rho_0 \bar{\lambda} (\Delta^2 \bar{\rho}_1 - \gamma \Delta^2 \partial_t \bar{\rho}_1),$$

$$\rho_0 \partial_t \Omega_1 + \rho_0 d_2 (\Omega_0 \cdot \nabla) \Omega_1 + d_3 P_{\Omega_0^\perp} \nabla \rho_1 = 0,$$

$$\Omega_0 \cdot \Omega_1 = 0, \bar{\lambda} = \frac{\rho_A}{\kappa \zeta}$$

- Consider plane wave perturbations

$$\rho_1(x, t) = \bar{\rho} e^{ik \cdot x + at}, \quad \Omega_1(x, t) = \tilde{\Omega} e^{ik \cdot x + at}$$

Linear stability analysis

- PDE system:

$$\partial_t \rho_g + \nabla \cdot \left((d_1 \Omega - \frac{1}{\zeta} \nabla \bar{\rho}_f - \frac{\mu}{\zeta} \nabla \rho_g) \rho_g \right) = 0,$$

$$\rho_g \partial_t \Omega + \rho_g \left((d_2 \Omega - \frac{1}{\zeta} \nabla \bar{\rho}_f - \frac{\mu}{\zeta} \nabla \rho_g) \cdot \nabla \right) \Omega + d_3 P_{\Omega^\perp} \nabla \rho_g = 0,$$

$$\rho_f = 1 + \frac{\gamma}{\eta} \Delta \bar{\rho}_g - \frac{\gamma^2}{\eta} \partial_t \Delta \bar{\rho}_g + \frac{\gamma^2}{\eta^2} \mathcal{N}(\bar{\rho}_g) + \mathcal{O}(\gamma^3),$$

- Linearize around (ρ_0, Ω_0) : $\rho_g = \rho_0 + \epsilon \rho_1 + \mathcal{O}(\epsilon^2)$, $\Omega = \Omega_0 + \epsilon \Omega_1 + \mathcal{O}(\epsilon^2)$

$$\partial_t \rho_1 + d_1 \Omega_0 \cdot \nabla \rho_1 + d_1 \rho_0 \nabla \cdot \Omega_1 = \bar{\mu} \rho_0 \Delta \rho_1 + \rho_0 \bar{\lambda} (\Delta^2 \bar{\rho}_1 - \gamma \Delta^2 \partial_t \bar{\rho}_1),$$

$$\rho_0 \partial_t \Omega_1 + \rho_0 d_2 (\Omega_0 \cdot \nabla) \Omega_1 + d_3 P_{\Omega_0^\perp} \nabla \rho_1 = 0,$$

$$\Omega_0 \cdot \Omega_1 = 0, \bar{\lambda} = \frac{\rho_A}{\kappa \zeta}$$

- Consider plane wave perturbations

$$\rho_1(x, t) = \tilde{\rho} e^{ik \cdot x + \alpha t}, \quad \Omega_1(x, t) = \tilde{\Omega} e^{ik \cdot x + \alpha t}$$

Linear stability analysis

Theorem (Bifurcation parameter)

The linearized system around (ρ_0, Ω_0) is unstable iff

$$b_p = \frac{\mu \kappa}{C_\phi^2 c_0'} < 1.$$

Characterisation of the most unstable modes:

Maximally disturbed modes :

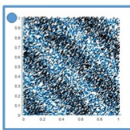
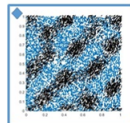
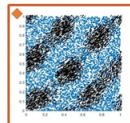
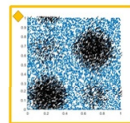
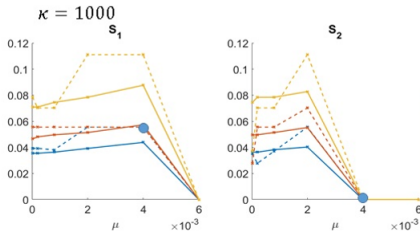
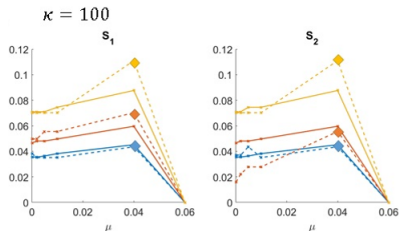
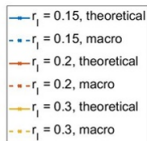
$$k_{\parallel}^{th} = \operatorname{argmax}_{k_{\parallel} \in \Omega_0} \operatorname{Re}(\tilde{\alpha}(k)),$$

$$k_{\perp}^{th} = \operatorname{argmax}_{k_{\perp} \in \Omega_0^{\perp}} \operatorname{Re}(\alpha(k)),$$

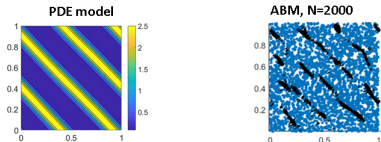
Related to size of perturbations

$$S_1^{th} = \frac{2\pi}{|k_{\parallel}^{th}|}, \quad S_2^{th} = \frac{2\pi}{|k_{\perp}^{th}|}.$$

Validation of the theoretical predictions (macro model)

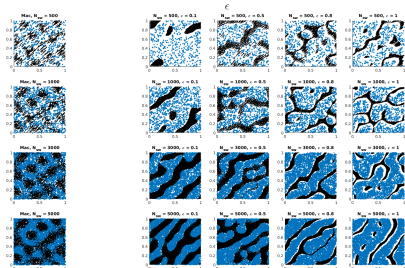
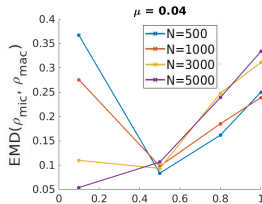
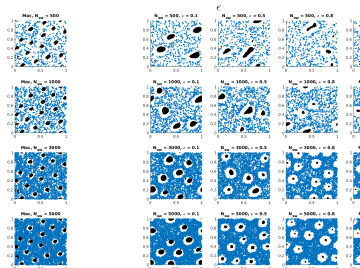
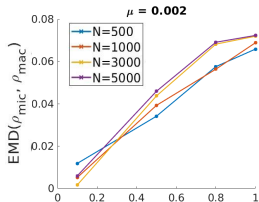


Micro-macro comparison



- Optimal Grid to compute the density of the ABM simulation (PIC method)
Must account for characteristic size of structures captured with finite number of points
- Distance independent of space translations
Wasserstein-type distance

Micro-macro comparison



Conclusions/perspectives

Conclusions

- Model for collective motion of active particles interacting in a viscoelastic medium
Variety of patterns depending on the interactions with the environment
- Attraction not required for swimmer aggregation
Obstacles can induce aggregation irrespective of whether they repel or attract the particles => rethink cause of biological aggregation
- Linear stability of PDE
Bifurcation parameter controlling the appearance and shape of patterns
- Micro-macro comparison
Quantitative agreement between ABM and PDE simulations

Perspectives

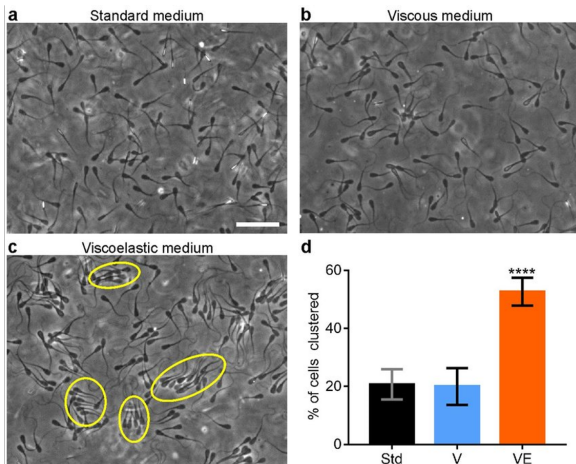
- Coupling with fluid model
- Different types of obstacles (elongated fibers)

[P. Aceves-Sanchez, P. Degond, E.E. Keaveny, A. Manhart, S. Merino-Aceituno, D. P., Large-scale dynamics of self-propelled particles moving through obstacles: model derivation and pattern formation. Bull. Math. Bio. (2020) 82(129)]

[P. Degond, A. Manhart, S. Merino-Aceituno, D. P., L. Sala, How environment affects active particle swarms: a case study, R. Soc. open sci (2022) 9:220791]

Thank you !

Collective motion: The role of the environment



Tung et al, Sci. Reports, 2017

Lemma 1 (Kinetic model)

Formally, as $N, M \rightarrow \infty$, $f^N \rightarrow f$ and $g^M \rightarrow g$ where $f(x, y, t)$ and $g(x, \alpha, t)$ fulfil:

$$\begin{aligned}\partial_t f + \nabla_x \cdot (\mathcal{W}f) &= d_0 \Delta_x f \\ \partial_t g + \nabla_x \cdot (\mathcal{U}g) + \nabla_\alpha \cdot (P_{\alpha^\perp} [\nu \bar{\alpha}]g) &= d_S \Delta_\alpha g,\end{aligned}$$

where

$$\bar{\alpha} = \frac{J_g(x, t)}{|J_g(x, t)|}, \quad J_g(x, t) = \int_{|x-z| \leq r_A} \alpha g(z, \alpha, t) dz d\alpha.$$

The velocities are given by

$$\begin{aligned}\mathcal{W} &= -\frac{\kappa}{\eta}(x - y) - \frac{1}{\eta} \nabla_x \bar{\rho}_g(x, t) \\ \mathcal{U} &= \alpha - \frac{1}{\zeta} \nabla_x \bar{\rho}_f(x, t) - \frac{1}{\zeta} \nabla_x \hat{\rho}_g(x, t),\end{aligned}$$

with

$$\bar{\rho}_g(x, t) = \int g(x, \alpha, t) d\alpha, \quad \bar{\rho}_f(x, t) = \int f(x, y, t) dy$$

and

$$\bar{\rho}(x, t) = \phi * \rho(x, t), \quad \hat{\rho}(x, t) = \psi * \rho(x, t)$$

Elements of proof for the hydrodynamic limit:

- Swimmer equation: Self-Organized Hydrodynamics:
Collision operator $Q(g) = -\nabla_\alpha \cdot (P_{\alpha\perp} [\nu \bar{\alpha}] g) + d \Delta_\alpha g$
[Degond, Motsch, 2008] (SOH)
[Degond, Dimarco, Mac, Wang, 2015] (SOHR)
- Obstacle equation:

$$\partial_t f + \nabla_x \cdot (\mathcal{W}f) = d_0 \Delta_x f, \quad \mathcal{W} = -\frac{\kappa}{\eta} (x - y) - \frac{1}{\eta} \nabla \bar{\rho}_g(x, t)$$

- Rewrite & rescale: $\gamma = \eta/\kappa$, $\delta = d_0 \gamma$ Fokker-Planck Operator

$$\partial_t f + \frac{1}{\eta} \nabla_x \cdot (-\nabla_x \bar{\rho}_g f) = \frac{1}{\gamma} \overbrace{[\nabla_x \cdot ((x - y)f + \delta \nabla_x f)]}$$

- Expand $f(x, y, t)$

$$f(x, y, t) = f_0(x, y, t) + \gamma f_1(x, y, t) + \gamma^2 f_2(x, y, t) + O(\gamma^3)$$

- Strong spring limit $\gamma \rightarrow 0$, small noise limit $\delta \rightarrow 0 \Rightarrow$ use Fokker-Planck Operator properties
- Gives $\rho_f(x, t)$ expanded in terms of γ and δ , $\rho_f(x, t) = \int f(x, y, t) dy$

Elements of proof for the hydrodynamic limit:

- Swimmer equation: Self-Organized Hydrodynamics:
Collision operator $Q(g) = -\nabla_\alpha \cdot (P_{\alpha\perp} [\nu\bar{\alpha}]g) + d\Delta_\alpha g$
[Degond, Motsch, 2008] (SOH)
[Degond, Dimarco, Mac, Wang, 2015] (SOHR)
- Obstacle equation:

$$\partial_t f + \nabla_x \cdot (\mathcal{W}f) = d_0 \Delta_x f, \quad \mathcal{W} = -\frac{\kappa}{\eta} (x - y) - \frac{1}{\eta} \nabla \bar{\rho}_g(x, t)$$

- Rewrite & rescale: $\gamma = \eta/\kappa$, $\delta = d_0\gamma$ Fokker-Planck Operator

$$\partial_t f + \frac{1}{\eta} \nabla_x \cdot (-\nabla_x \bar{\rho}_g f) = \frac{1}{\gamma} \overbrace{[\nabla_x \cdot ((x - y)f + \delta \nabla_x f)]}^{\text{Fokker-Planck Operator}}$$

- Expand $f(x, y, t)$

$$f(x, y, t) = f_0(x, y, t) + \gamma f_1(x, y, t) + \gamma^2 f_2(x, y, t) + O(\gamma^3)$$

- Strong spring limit $\gamma \rightarrow 0$, small noise limit $\delta \rightarrow 0 \Rightarrow$ use Fokker-Planck Operator properties
- Gives $\rho_f(x, t)$ expanded in terms of γ and δ , $\rho_f(x, t) = \int f(x, y, t) dy$

Elements of proof for the hydrodynamic limit:

- Swimmer equation: Self-Organized Hydrodynamics:
Collision operator $Q(g) = -\nabla_\alpha \cdot (P_{\alpha\perp} [\nu\bar{\alpha}]g) + d\Delta_\alpha g$
[Degond, Motsch, 2008] (SOH)
[Degond, Dimarco, Mac, Wang, 2015] (SOHR)
- Obstacle equation:

$$\partial_t f + \nabla_x \cdot (\mathcal{W}f) = d_0 \Delta_x f, \quad \mathcal{W} = -\frac{\kappa}{\eta} (x - y) - \frac{1}{\eta} \nabla \bar{\rho}_g(x, t)$$

- Rewrite & rescale: $\gamma = \eta/\kappa$, $\delta = d_0\gamma$ Fokker-Planck Operator

$$\partial_t f + \frac{1}{\eta} \nabla_x \cdot (-\nabla_x \bar{\rho}_g f) = \frac{1}{\gamma} \overbrace{[\nabla_x \cdot ((x - y)f + \delta \nabla_x f)]}^{\text{Fokker-Planck Operator}}$$

- Expand $f(x, y, t)$

$$f(x, y, t) = f_0(x, y, t) + \gamma f_1(x, y, t) + \gamma^2 f_2(x, y, t) + O(\gamma^3)$$

- Strong spring limit $\gamma \rightarrow 0$, small noise limit $\delta \rightarrow 0 \Rightarrow$ use Fokker-Planck Operator properties
- Gives $\rho_f(x, t)$ expanded in terms of γ and δ , $\rho_f(x, t) = \int f(x, y, t) dy$

Elements of proof for the hydrodynamic limit:

- Swimmer equation: Self-Organized Hydrodynamics:
Collision operator $Q(g) = -\nabla_\alpha \cdot (P_{\alpha\perp} [\nu\bar{\alpha}]g) + d\Delta_\alpha g$
[Degond, Motsch, 2008] (SOH)
[Degond, Dimarco, Mac, Wang, 2015] (SOHR)
- Obstacle equation:

$$\partial_t f + \nabla_x \cdot (\mathcal{W}f) = d_0 \Delta_x f, \quad \mathcal{W} = -\frac{\kappa}{\eta} (x - y) - \frac{1}{\eta} \nabla \bar{\rho}_g(x, t)$$

- Rewrite & rescale: $\gamma = \eta/\kappa$, $\delta = d_0\gamma$ Fokker-Planck Operator

$$\partial_t f + \frac{1}{\eta} \nabla_x \cdot (-\nabla_x \bar{\rho}_g f) = \frac{1}{\gamma} \overbrace{[\nabla_x \cdot ((x - y)f + \delta \nabla_x f)]}^{\text{Fokker-Planck Operator}}$$

- Expand $f(x, y, t)$

$$f(x, y, t) = f_0(x, y, t) + \gamma f_1(x, y, t) + \gamma^2 f_2(x, y, t) + O(\gamma^3)$$

- Strong spring limit $\gamma \rightarrow 0$, small noise limit $\delta \rightarrow 0 \Rightarrow$ use Fokker-Planck Operator properties
- Gives $\rho_f(x, t)$ expanded in terms of γ and δ , $\rho_f(x, t) = \int f(x, y, t) dy$

Substituting the plane wave ansatz into the equation yields

$$\tilde{\rho}\alpha + i\tilde{\rho}d_1(\Omega_0 \cdot k) + i\rho_0d_1(\tilde{\Omega} \cdot k) = -|k|^2\bar{\mu}\rho_0\tilde{\rho} + |k|^4\bar{\lambda}\rho_0\tilde{\rho}(\hat{\phi}_k)^2(1 - \gamma\alpha), \quad (1a)$$

$$\rho_0\alpha\tilde{\Omega} + i\rho_0d_2\tilde{\Omega}(\Omega_0 \cdot k) + i\tilde{\rho}d_3P_{\Omega_0^\perp}k = 0, \quad (1b)$$

$$\Omega_0 \cdot \tilde{\Omega} = 0. \quad (1c)$$

or (if $\tilde{\Omega} = \omega\Omega_0^\perp$)

$$\begin{aligned} (G(|k|)\alpha - F(|k|) + id_1k_0)\tilde{\rho} + i\rho_0d_1k_1\omega &= 0, \\ id_3k_1\tilde{\rho} + \rho_0(\alpha + id_2k_0)\omega &= 0. \end{aligned}$$

This is a homogeneous linear system in $(\tilde{\rho}, \omega)$ which has a non-trivial solution if and only if the determinant of the system is 0, *i.e.*:

$$(G(|k|)\alpha - F(|k|) + id_1k_0)(\alpha + id_2k_0) + d_1d_3k_1^2 = 0. \quad (2)$$

Linear stability analysis

Theorem (Bifurcation parameter)

Consider fixed constant values $\rho_0 > 0$ and $\Omega_0 \in \mathbb{S}^1$. Then, the linearized system around (ρ_0, Ω_0) is unstable if and only if

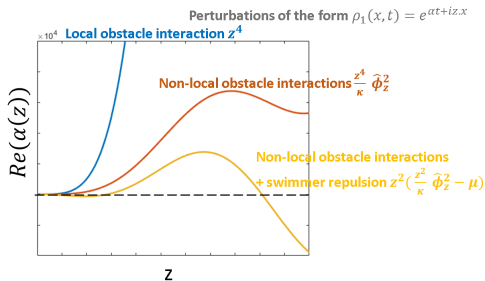
there exists $z > 0$ such that $z^2(\hat{\phi})^2 > \mu\kappa$.

Obstacle interaction function:

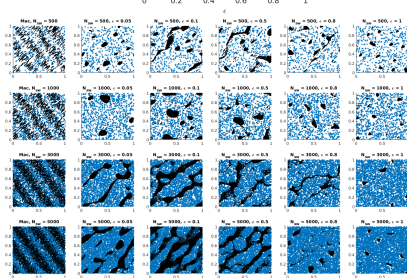
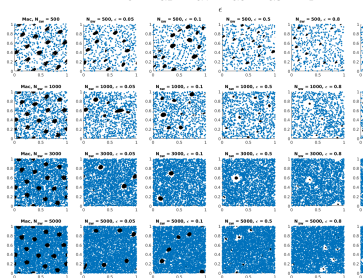
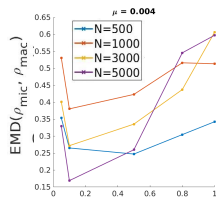
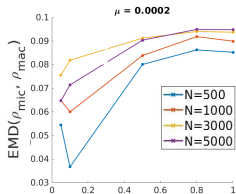
$$\phi(x) = \frac{3C_\phi}{2\pi\tau} \left(1 - \frac{|x|}{\tau}\right)_+^2$$

Real part of $\alpha(z)$:

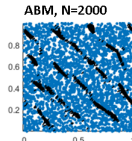
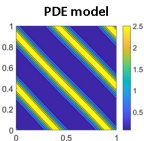
$$\text{Re}(\alpha(z)) = \frac{\rho_0}{\zeta} z^2 \left[\frac{z^2}{\kappa} \hat{\phi}_z^2 - \mu \right]$$



Micro-macro comparison

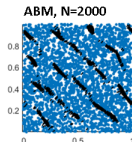
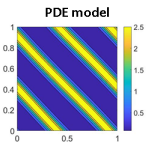


Micro-macro comparison

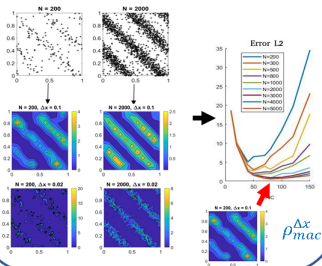


- Optimal Grid to compute the density of the ABM simulation (PIC method)
Must account for characteristic size of structures captured with finite number of points
- Distance independent of space translations
Wasserstein-type distance

Micro-macro comparison



1. Choose the best grid for macro simulation



Micro-macro comparison

